Biophysical Journal Volume 89 November 2005 3577–3588

I-Domain of Lymphocyte Function-Associated Antigen-1 Mediates Rolling of Polystyrene Particles on ICAM-1 under Flow

A. Omolola Eniola,*‡ Ellen F. Krasik,†‡ Lee A. Smith,*‡ Gang Song,§ and Daniel A. Hammer*†‡

*Department of Chemical and Biomolecular Engineering, †Department of Bioengineering, and ‡Institute for Medicine and Engineering, University of Pennsylvania, Philadelphia, Pennsylvania 19104; and §CBR Biomedical Research Institute, Harvard Medical School, Boston, Massachusetts 02115

ABSTRACT In their active state, β_2-integrins, such as LFA-1, mediate the firm arrest of leukocytes by binding intercellular adhesion molecules (ICAMs) expressed on endothelium. Although the primary function of LFA-1 is assumed to be the ability to mediate firm adhesion, recent work has shown that LFA-1 can contribute to cell tethering and rolling under hydrodynamic flow, a role previously largely attributed to the selectins. The inserted (I) domain of LFA-1 has recently been crystallized in the wild-type (wt) and locked-open conformations and has been shown to, respectively, support rolling and firm adhesion under flow when expressed in $\alpha_L\beta_2$ heterodimers or as isolated domains on cells. Here, we report results from cell-free adhesion assays where wt I-domain-coated polystyrene particles were allowed to interact with ICAM-1-coated surfaces in shear flow. We show that wt I-domain can independently mediate the capture of particles from flow and support their rolling on ICAM-1 surfaces in a manner similar to how carbohydrate-selectin interactions mediate rolling. Adhesion is specific and blocked by appropriate antibodies. We also show that the rolling velocity of I-domain-coated particles depends on the wall shear stress in flow chamber, I-domain site density on microsphere surfaces, and ICAM-1 site density on substrate surfaces. Furthermore, we show that rolling is less sensitive to wall shear stress and ICAM-1 substrate density at high density of I-domain on the microsphere surface. Computer simulations using adhesive dynamics can recreate bead rolling dynamics and show that the mechanochemical properties of ICAM-1-I-domain interactions are similar to those of carbohydrate-selectin interactions. Understanding the biophysics of adhesion mediated by the I-domain of LFA-1 can elucidate the complex roles this integrin plays in leukocyte adhesion in inflammation.

INTRODUCTION

Inflammation, a natural process by which living tissues respond to injury, is often accompanied by changes in blood flow, increased permeability of blood vessels, and adhesion and migration of leukocytes from blood into tissues. Leukocyte adhesion to the endothelium and transendothelial migration in response to inflammatory stimuli occur via multiple receptor-ligand interactions (1). The endothelial selectins (P- and E-selectin) can mediate the initial, transient (rolling) adhesion of leukocytes onto the endothelium via interaction with their counterreceptors expressed on leukocyte cell surfaces (1,2). This rolling adhesion is a prerequisite for the firm arrest of leukocytes to the endothelium that is mediated by activated leukocyte β_2-integrins binding to endothelial-expressed intercellular adhesion molecules (ICAMs) (2–5). β_2-integrins are also believed to be involved in the transendothelial migration of leukocytes that follows their firm arrest onto the endothelium, though platelet endothelial cell adhesion molecule-1 (PECAM-1) is also thought to play a major role in extravasation (6,7). Lymphocyte function-associated antigen-1 (LFA-1) is the primary β_2-integrin involved in the firm arrest of leukocytes to the vascular wall during the inflammatory response (8), and ICAM-1 is the major endothelial adhesion ligand to LFA-1. LFA-1, also known as $\alpha_L\beta_2$, is constitutively expressed on leukocyte surface in a low affinity state but can switch to a high affinity state upon receiving signals transmitted from within leukocytes after receptor binding or activation (1,9). The precise contribution of LFA-1 before activation is unclear. The lymphocyte integrin $\alpha_4\beta_1$ can exist in two states and in the low affinity state can support rolling and in the high affinity state can support firm adhesion (10). Whether LFA-1 can support or supplement adhesion in the low affinity state has perhaps been occluded by its coexpression with leukocyte selectins. Recent work shows that LFA-1, along with other β_2-integrins such as Mac-1, has a role in stabilizing selectin-mediated rolling interaction, resulting in slow leukocyte rolling on inflamed endothelium in vivo (11–15).

To understand LFA-1 affinity regulation and its effect on leukocyte adhesion, researchers have focused attention on the adhesion domains in LFA-1. Three domains, inserted (I), β-propeller, and I-like domain, located in the headpiece of LFA-1 have been suggested to be involved in ligand binding or in the regulation of ligand binding (16); however, the I-domain serves as the primary ICAM-1 binding site on LFA-1. This domain has recently been crystallized in the intermediate and open conformation (closed conformation was crystallized earlier by Qu and Leahy (17)); and affinity measurements show that the closed conformation has low affinity

Submitted December 8, 2004, and accepted for publication July 21, 2005.

Address reprint requests to Daniel A. Hammer, Dept. of Bioengineering, University of Pennsylvania, 120 Hayden Hall, 3320 Smith Walk, Philadelphia, PA 19104. Tel.: 215-573-6761; Fax: 215-573-2071; E-mail: hammer@seas.upenn.edu.

0006-3495/05/11/3577/12 $2.00

doi: 10.1529/biophysj.104.057729

to ICAM-1, similar to wild-type (wt) I-domain, whereas the open conformation has a high affinity to ICAM-1 (18).

The notion that I-domain can support rolling is supported by experiments in which the low affinity (wt) state, expressed on cells in isolation from other domains, can support rolling adhesion on ICAM-1 surfaces under shear flow in vitro (10,19). Other work has shown that LFA-1 as an intact molecule on cell surfaces can also support rolling adhesion on ICAM-1 in shear flow separate from, but similar to, selectin-mediated rolling adhesion (20). Although these studies show the ability of low affinity LFA-1 and its I-domain to form and maintain transient adhesion, they do not fully explore their ability to mediate cell tethering from flow since the initial contact between LFA-1/I-domain-expressing cells and ICAM-1 substrates occurred at very low shear rate or in the absence of flow (i.e., cells were allowed to settle on substrate before initiating flow (20)). In addition, they do not allow the ability to vary systematically the density of I-domain molecules and study the effects on rolling dynamics and tethering.

Here, we illustrate the ability of wt I-domain to mediate tethering and maintain stable rolling in a cell-free in vitro flow system up to physiological shear rates. We also explore the effect of molecule (I-domain and ICAM-1) density on rolling dynamics. To do this, purified I-domain was attached to the surface of polystyrene microspheres via avidin-biotin linkage; and after I-domain attachment, particles were allowed to interact with ICAM-1 surfaces under flow. We show that I-domain can independently mediate the capture of particles from flow and support their rolling on ICAM-1 surfaces, in a fashion similar to that displayed by carbohydrate-selectin interactions in a cell-free system (21). Rolling is specific and blocked by appropriate antibodies. We also show that the rolling velocity of I-domain particles depends on the wall shear stress in the flow chamber, I-domain site density on microspheres and ICAM-1 site density on the substrate surface. Furthermore, we show that rolling is less sensitive to wall shear stress and ICAM-1 substrate density at a high density of I-domain on microsphere surfaces. An analysis of rolling dynamics using adhesive dynamics (AD) suggests that the off rate and reactive compliance for I-domain-ICAM-1 interactions are 4 s^{-1} and 0.1 Å, respectively, rather close to the values of these parameters for selectin-carbohydrate interactions and well within the rolling envelop in the state diagram relating mechanicochemical properties of adhesion molecules to rolling (22). Therefore, our findings support the notion that I-domain (and LFA-1) can act as a rolling ligand in tandem with selectin interactions before leukocyte and integrin activation. The overall purpose of this work is to further understand the contribution of LFA-1 to the transition from rolling to firm arrest that must occur for neutrophils and other leukocytes to marginate into tissues during inflammation response by elucidating the biophysics of the adhesion mediated by the inserted- (I)-domain that is known to be a major adhesion domain on LFA-1.

MATERIALS AND METHODS

Adhesion molecules and antibodies

Recombinant human ICAM-1/Fc chimera (mouse IgG1) and anti-ICAM-1 monoclonal antibody (mAb) BBIG-I1 were purchased from R & D Systems (Minneapolis, MN). Fluorosceine Iso-thio-cyanate (FITC)-labeled anti-mouse IgG1 was purchased from Pharmingen (San Diego, CA). Sialyl $Lewis^X$ carbohydrate (sLe^X) was purchased from Glycotech (Rockville, MD). Anti-human α_L I-domain monoclonal antibodies, TS1/11, TS1/12, and TS2/6 were previously described (23,24).

Construction and expression of biotinylated wt LFA-1 I-domain

A BirA enzyme recognition tag (LGGIFEAMKMELRD) was fused to the N-terminal of wt α_L I-domain ($Gly^{128-Y307}$) through Gly-Gly-Gly-Ser linker (18,25–27). The cDNA was cloned into the *Nde*I and *Bam*HI sites of the pET-20b vector. Protein was expressed in *Escherichia coli* BL21 DE3 (Novagen, La Jolla, CA). The transformed bacteria were cultured in rich media (20 g/L tryptone, 10 g/L yeast extract, 5 g/L NaCl, 20 ml/L glycerol, 50 mM K_2HPO4, 10 mM $MgCl_2$, 10 g/L glucose, 100 mg/L ampicillin). The expression was induced by addition of isopropyl α-D-thiogalactopyranoside (IPTG) (Invitrogen, Carlsbad, CA) to a final concentration of 1 mM at OD600 nm of 0.6–1.0. After 3 h of induction at 37°C, bacteria were harvested by centrifugation and frozen at −20°C. Frozen cells were resuspended in Tris buffered saline (TBS) with 1 mg/mL lysozyme and then disrupted by ultrasonication. Inclusion bodies were harvested by centrifugation. After extensive washing with washing buffer (20 mM Tris (pH 8.0), 23% (w/v) sucrose, 0.5% (v/v) Triton X-100, 1 mM EDTA), the pellet was solubilized by adding 6 M Guanidine HCl, 50 mM Tris (pH 8.0), 1 mM Dithiothreitol (DTT). I-domain was refolded in TBS-glycerol buffer (20 mM Tris (pH 8.0), 100 mM NaCl, 5% glycerol) and then purified by Superdex S-200 (Amersham Biosciences, Piscataway, NJ) gel-filtration in phosphate-buffered saline (PBS) after ammonium sulfate precipitation. Site-directed biotinylation was performed using the BirA enzyme (Avidity, Denver, CO). Typically, I-domain at concentrations of 1–2 mg/ml was incubated with BirA (15–20 μg/ml) at room temperature overnight in a buffer containing 20 mM Tris (pH 8.0), 100 mM NaCl, 10 mM $MgOAc_2$, 50 mM Bicine (pH 8.3), 10 mM ATP, and 50 μM biotin. The unbound biotin was completely removed by passing the sample through a Superdex S-200 column (Amersham) in a running buffer (20 mM Tris (pH 8.0), 150 mM NaCl).

Substrate preparation

ICAM-1 surfaces were prepared as previously described (28). Briefly, double-well, rectangular flexiperm gaskets were placed on microscope slides cut from bacteriological polystyrene dishes. The surface enclosed by one of the two wells was incubated overnight with 374 μL ICAM-1 in binding buffer (0.1 M $NaHCO_3$) at 1.25, 2.5, or 5 μg/mL (sample) and the other with binding buffer only (control). After incubation, slides were washed and blocked for 1 h with 2% solution of denatured bovine serum albumin (BSA) in Dulbecco's phosphate-buffered saline (DPBS). Before use in laminar flow, slides were incubated with 1% Tween 20 in DPBS for ~2 min. ICAM-1 density determination was as previously described (28). Briefly, eight-well, rectangular, flexiperm gaskets on polystyrene slides were incubated with ICAM-1 at desired concentrations and blocked with BSA similar to flow experiment. ICAM-1-coated wells were then incubated with a saturating concentration of FITC-labeled aICAM-1 mAb (BBIG-I1). Fluorescence intensity was obtained using FeliX software (Photon Technologies, Severna Park, MD) and a Nikon Diaphot inverted microscope (Melville, NY) equipped with a FITC cube. ICAM-1 site density (molecules/μm^2) was obtained using calibration curves generated by measuring the fluorescence of known concentration of FITC-aICAM-1.

Microsphere preparation

Biotinylated I-domain and sLe^X were diluted to 5 μg/mL in $DPBS^+$ (DPBS, 1% BSA, 1 mM Ca^{2+}, 2 mM Mg^{2+}, pH = 7.4). These two solutions were then mixed at ratios between 0% and 100% I-domain. A total of 10^6 SuperAvidin-coated beads (~10 μm, 1.060 g/cm^3, Bangs Laboratories, Fishers, IN) were coated with 100 μL of solutions containing both I-domain and sLe^X at different ratios for 1 h at room temperature. Since a microsphere-coating concentration of 5 μg/mL is saturating, adding a non-ICAM-1 functional molecule, like sLe^X, in the coating solution to compete for biotin binding sites on microspheres can guarantee a significant reduction in I-domain site density with a decrease in the amount of I-domain in coating solution. Control beads were prepared by coating microspheres with 100 μL sLe^X solution at 5 μg/mL. After incubation, beads were washed twice in $DPBS^+$ and resuspended in 2 mL $DPBS^+$ until ready for use.

Microsphere I-domain site density determination

Three different anti-human α_L I-domain mAbs, TS1/11, TS1/12, and TS2/6, were used to determine surface density of wt I-domain on microsphere surface (10). Briefly, 10^5 I-domain-coated microspheres were incubated with 100 μL of primary antibody (20 μg/mL in $DPBS^+$) for 1 h. After primary antibody incubation, beads were washed twice in $DPBS^+$ and incubated with 100 μL of FITC-labeled anti-mouse IgG_1 mAb (30 μg/mL). Fluorescence intensity was measured using flow cytometry, and I-domain site density was estimated as previously described (29). Briefly, fluorescence shifts of I-domain particles were converted to molecules of equivalent soluble fluorochrome (MESF) using a calibration curve relating mean peak fluorescence of Quantum 26 calibration beads (Bangs Laboratories) to their MESF. The number of surface-bound I-domain was determined by converting the corresponding MESF value of I-domain particles to site density using the fluorochrome/protein ratio of FITC-conjugated secondary antibody and assuming a 1:1 binding between the I-domain and the primary and the secondary antibody.

Laminar flow assay

A straight-channel, parallel-plate flow chamber was used for laminar flow assays. Briefly, a straight channel template was placed over an ICAM-1-coated slide. The template and slide were then placed in the bottom well of the flow chamber. The flow chamber experiment was as previously described (21,29), where the assembled chamber was mounted on the stage of a Nikon Diaphot inverted microscope with phase-contrast optics (Nikon, Tokyo, Japan). A bead concentration of 10^6 I-domain-coated or sLe^X-coated microspheres in 2 mL $DBPS^+$ was used, and flow was initiated with an infusion/withdrawal syringe pump (Harvard Apparatus, South Natick, MA). Experiments were recorded using a Cohu black and white charge-coupled device camera (Cohu, San Diego, CA) and a Sony SVO-9500MD S-VHS recorder (Sony Medical Systems, Montvale, NJ). Wall shear stress in flow chamber (τ_w) was calculated as previously described (29). To confirm the dependence of I-domain-ICAM-1 interaction on divalent cations, Ca^{2+} and Mg^{2+}, 10 mM EDTA was added to perfusion buffer ($DPBS^+$) to remove these ions.

Data analysis

Rolling velocities were obtained through digital image analysis of video records of adhesion experiments using LabView software (National Instrument, Austin, TX), and the average rolling velocities were obtained by taking the mean velocity of at least 10 particles continuously rolling for 3 s or longer (21). Rolling is defined as particles moving <10% of free stream velocity. Rolling flux of interacting beads was obtained manually by counting the number of rolling beads in the window of view (0.32 mm^2) over a period of 1 min. Instantaneous rolling velocities (V_{inst}) were determined by dividing the displacement of particle by the time between captured frames. V_{inst} data were obtained every one-sixth of a second. The standard deviation of the instantaneous rolling velocity, root mean-square rolling velocity (V_{rms}), of each particle was calculated as previously described (30). Unless otherwise stated, error bars were plotted using standard error calculation. Data plots show the average of at least three experiments. Differences in the level of adhesion for the different conditions tested were examined using two-tailed Student's t-test. A value of $p < 0.05$ was considered statically significant.

Adhesive dynamics

The AD method that has been previously described was used to analyze the rolling dynamics of I-domain-ICAM-1 interactions (22,31,32). Briefly, AD simulates the adhesive behavior of a rigid sphere (i.e., bead or model cell) in near contact with a wall (i.e., slide or endothelium) under shear flow. At each time step, a contact zone is defined between the bead and the uniformly reactive planar surface, and randomly distributed cell-surface receptors within that zone are tested for bond formation according to probabilities calculated from bond-length-dependent kinetic rates. All preexisting bonds are then tested for breakage, also according to bond-length-dependent rates. If a bond forms, over its lifetime it is represented by a linear spring whose endpoints remain fixed with respect to either surface. The orientation and length of each spring specifies the instantaneous force and torque exerted by that bond on the sphere and also its probability for breakage per unit time. A summation of external forces and torques due to bonds, gravity, and nonspecific steric repulsion enables a mobility calculation to determine the translational and rotational velocities of the sphere under flow. For a single particle in low Reynolds number Couette flow, the mobility function is available as a closed-form solution for all modes of motion (31,33,34). Finally, cell and bond positions are updated according to the kinematics of cell motion, neglecting inertia and assuming velocities to be constant over each time step of 0.1 μs. This process is repeated until 10 s of simulation time have elapsed. Each reported average rolling velocity represents the averaged results of $n \geq 7$ realizations.

Calculation of the probability of breakage, $P_r = 1 - \exp(k_r \Delta t)$, employs the Bell model describing the kinetics of single biomolecular bond failure (35),

$$k_r = k_r^0 \exp\left(\frac{\gamma \sigma |x_b - \lambda|}{\kappa_B T}\right), \quad (1)$$

which relates the rate of dissociation k_r to the magnitude of the force on the bond, calculated using the Hookean spring constant σ, and deviation bond length $|x_b - \lambda|$, where x_b is the bond length and λ is the unstressed, equilibrium bond length. The unstressed off rate k_r^0 and reactive compliance γ have been determined experimentally for LFA-1-ICAM-1 bonds using atomic force microscopy measurements (36). BIAcore measurements have yielded values of k_r^0 for the α_L integrin I-domain-ICAM-1 interactions (18).

Once the rate of dissociation is set by Eq. 1, the rate of formation directly follows from the Boltzmann distribution for affinity (37),

$$k_f = k_f^0 \exp\left[\sigma \left| y - \lambda \left(\gamma - \frac{1}{2}|x_b - \lambda|\right)\right| \Big/ K_B T\right], \quad (2)$$

permitting the calculation of the probability of bond formation $P_f = 1 - \exp(k_f \Delta t)$. The two-dimensional intrinsic on rate k_f^0 of the I-domain-ICAM-1 bond, whose molecular participants are fixed on respective surfaces, has not been measured experimentally and remains a tunable parameter. The expression for the overall forward binding rate is also a function of the wall surface ligand density and the relative velocity between the two surfaces, exhibiting a first-order dependence on the Peclet number (38). Physical parameters used in the simulation are listed in Table 1.

TABLE 1 Values of physical parameters used in simulations

Parameter	Definition	Value	Reference
a	Particle radius	5 μm	(46)
μ	Viscosity	0.01 P	
ρ	Fluid density	1 g/cm^3	
$\Delta\rho$	Density difference	0.05 g/cm^3	
λ	Equilibrium bond length	70 nm	(47)
σ	Spring constant	100 dyn/cm	(48)
T	Temperature	298 K	
k_f^0	Intrinsic on rate	0.3 μm^2/s	
γ	Reactive compliance	0.1 Å	
k_r^0	Unstressed off rate	4.0 s^{-1}	

TABLE 2 Average I-domain site density (sites/μm^2) on microsphere surface for TS2/6, TS1/11, and TS1/12 staining

Coating concentration (μg/ml I-domain)	Average I-domain site density (sites/μm^2)	Standard error
0	0	0
1.5	94	12
2.5	252	15
3.5	824	49
5.0	1731	165

RESULTS

I-domain density on microspheres

Microsphere I-domain site densities were determined by flow cytometry. Fig. 1 shows the fluorescence histograms obtained for I-domain-coated microspheres stained with primary antibody TS2/6 (~20 μg/mL). The control histogram represents microspheres coated with sLe^X only. Rightward shift in fluorescence intensity of I-domain-coated beads from control confirms the presence of I-domain on the microsphere surface. As shown in Fig. 1, the shift in fluorescence intensity from control beads increased with increasing I-domain concentration in solution. Fluorescence intensity data were related to molecular density using fluorescent calibration beads. Table 2 lists the average I-domain density on the microsphere surface obtained from flow cytometry measurements with all three antibodies, TS1/11, TS1/12, and TS2/6, anti-human α_L I-domain mAbs. Microspheres coated with 2.5 μg/ml I-domain in solution resulted in an I-domain site density of 252 $\pm$ 15 sites/μm^2 on the microsphere surface. This site density is similar to the amount of β_2-integrin, ~300 sites/μm^2, on resting neutrophils (based on an apparent surface area of 227 μm^2) (39,40).

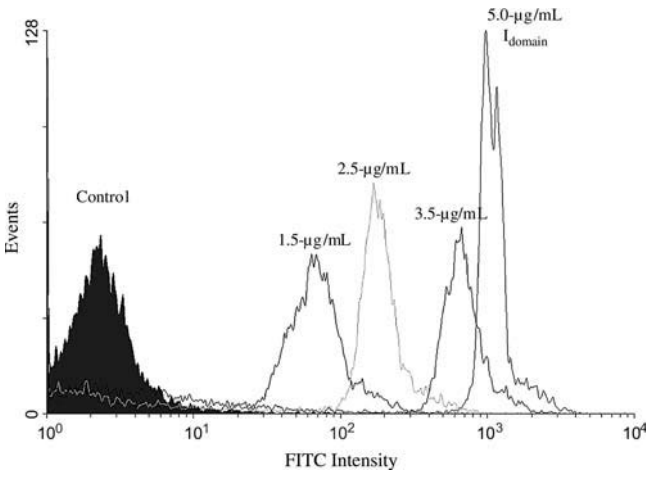

FIGURE 1 Fluorescence histogram for SuperAvidin microspheres (9.95 μm) incubated with 5 μg/mL solutions containing 0% (control), 30%, 50%, 70%, and 100% I-domain. Primary antibody: TS2/6 (1:10 dilution). Secondary antibody: FITC-labeled anti-mouse IgG (25 μg/mL).

Wt I-domain specifically mediates the dynamic adhesion of microspheres on ICAM-1 substrate

I-domain-coated particles were allowed to interact with the ICAM-1-coated surface in continuous laminar shear flow in a parallel plate flow chamber. Wt I-domain mediated the capture of polystyrene microspheres from free stream and maintained slow rolling of these microspheres on ICAM-1. Fig. 2 shows rolling and firm binding flux of microspheres on surfaces with ~210 sites/μm^2 ICAM-1 at a wall shear stress of ~1.3 dynes/cm^2. Firm adhesion of microspheres was not observed with any of the I-domain site densities or ICAM-1 surface densities studied. In addition, microspheres coated with only sLe^X (5 μg/mL) did not roll on or firmly adhere to ICAM-1 surfaces, and microspheres coated with anti-ICAM-1 mAb (BBIG-I1) showed no rolling and only firm adhesion on ICAM-1 (data not shown). The presence of EDTA in the perfusion buffer abolished rolling interaction between I-domain particles and ICAM-1 surfaces (Fig. 2). Control experiments with the anti-human α_L mAb TS 2/6

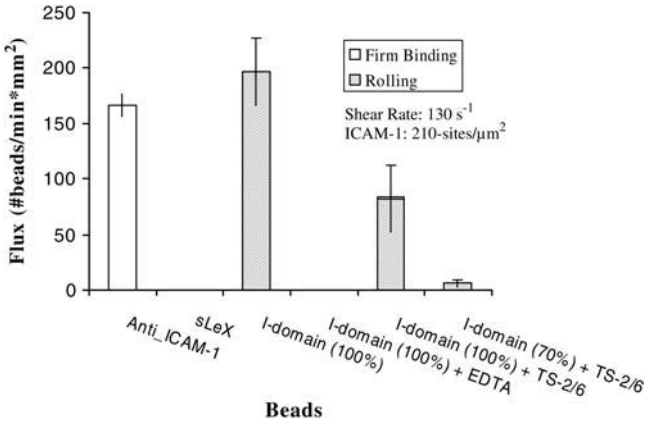

FIGURE 2 Rolling and binding flux of beads coated with 1730 (100%) and 824 (70%) sites of I-domain, 2800 sites/μm^2 of anti-ICAM-1 (100%), and 1321 sites/μm^2 of sLe^X (100%) on 210 sites/μm^2 ICAM-1 surfaces ($n \geq 4$) at 130 s^{-1}. Beads were suspended in PBS$^+$ (1% BSA, 1 mM Ca^{2+}, 2 mM Mg^{2+}). The experiment with EDTA was with PBS$^+$ w/o ions. Field of view = 0.32 mm^2, time = 1 min, and TS2/6 concentration = ~20 μg/mL. *Baseline flux = 264 beads/mm$^2\times$min.

significantly reduced the level of rolling adhesion with I-domain beads on ICAM-1.

Rolling adhesion of microspheres is a function of I-domain site density, ICAM-1 substrate density, and wall shear stress in flow chamber

Average rolling velocities for I-domain-coated microspheres on ICAM-1 were measured at different microsphere and substrate molecule densities and wall shear stresses. Fig. 3 shows the microsphere rolling velocity as a function of wall shear stress at different I-domain microsphere and ICAM-1 surface densities. At a given ICAM-1 substrate density, microsphere rolling velocity decreases with increasing microsphere I-domain site density for all shear stress studied. The sensitivity of rolling velocity to I-domain density appears to increase with increasing wall shear stress within the flow chamber (see Fig. 3 *A*, *inset*) and decreasing ICAM-1 substrate density. Similarly, at a given I-domain site density, rolling velocity decreases with increasing ICAM-1 site density at all shear stresses (e.g., compare *squares* in Fig. 3, *A–C*; $P < 0.05$). As also shown in Fig. 3, the rolling velocity of I-domain microspheres increased significantly with an increase in the wall shear within the flow chamber at most I-domain and ICAM-1 densities studied, and the magnitude of increase depended on the I-domain and ICAM-1 density.

To further elucidate the apparent coupling effect of shear stress and density of adhesion molecules on rolling velocity, we present rolling velocity data in contour plots. Fig. 4 shows the contour plots of I-domain microsphere rolling velocity at different shear stresses within the flow chamber for different microsphere and substrate molecular densities. In Fig. 4 *A*, rolling velocity progressively becomes insensitive to wall shear stress as the I-domain site density on microspheres increased. Similarly, Fig. 4 *B* shows a region, at low wall shear stress and high ICAM-1 density, where rolling velocity is insensitive to shear stress.

Instantaneous rolling velocity and its fluctuation with time

Instantaneous rolling velocities of I-domain-coated microspheres on ICAM-1 surfaces were calculated as described in Materials and Methods. Fig. 5 shows representative instantaneous rolling velocity traces for I-domain microspheres at different I-domain and ICAM-1 site densities and at different wall shear stresses. The velocities with which wt I-domain particles interacted with ICAM-1 surfaces vary with time at all conditions studied. These particles also displayed brief pauses (periods of zero velocity) when interacting with ICAM-1 substrates. Furthermore, the amount of time paused and the duration of pausing decreased with a decrease in I-domain or ICAM-1 densities on microspheres or substrate

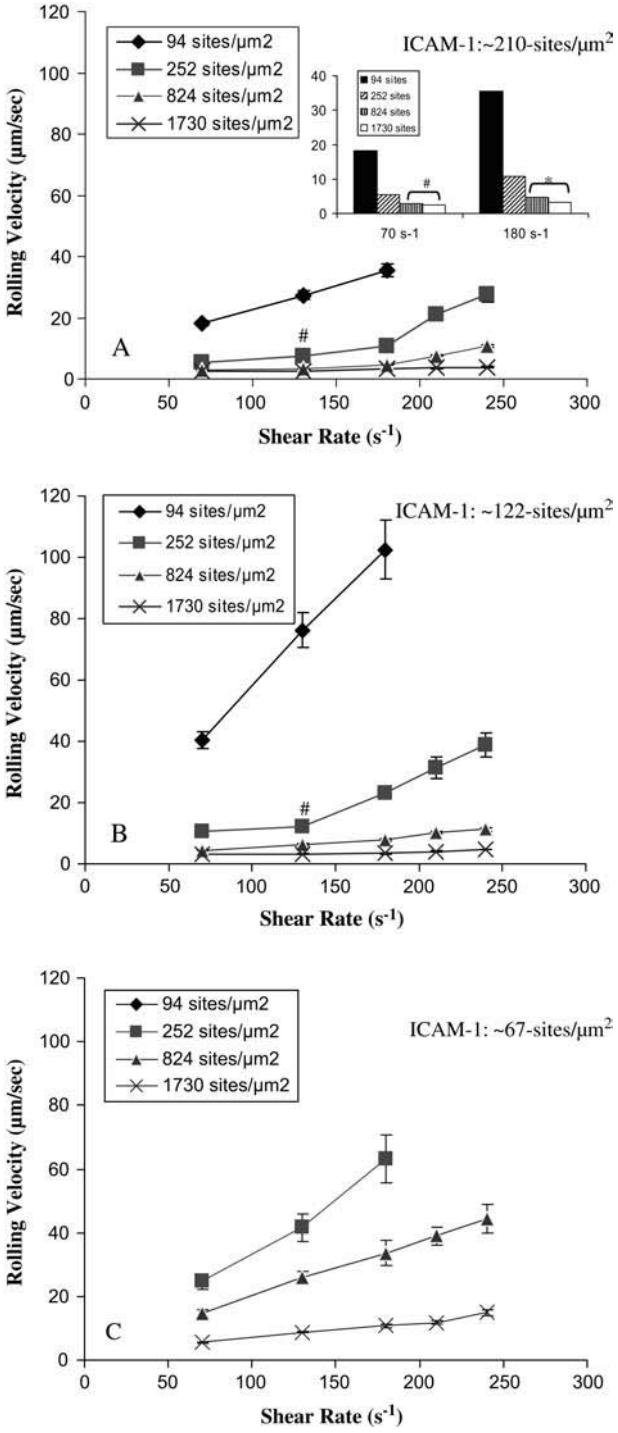

FIGURE 3 Rolling velocity as a function of wall shear rate for I-domain microspheres on surfaces coated with (*A*) 1.25, (*B*) 2.5, and (*C*) 5.0 μg/mL of ICAM-1. Beads were suspended in PBS^+ (1% BSA, 1 mM Ca^{2+}, 2 mM Mg^{2+}). Error bars = standard error ($n \geq 4$); #no significant increase from previous shear rate ($P > 0.05$). (*Inset*) (*A*) Rolling velocity of I-domain microspheres at 70 s^{-1} and 180 s^{-1} shear rates (*$P < 0.0001$, #$P > 0.05$).

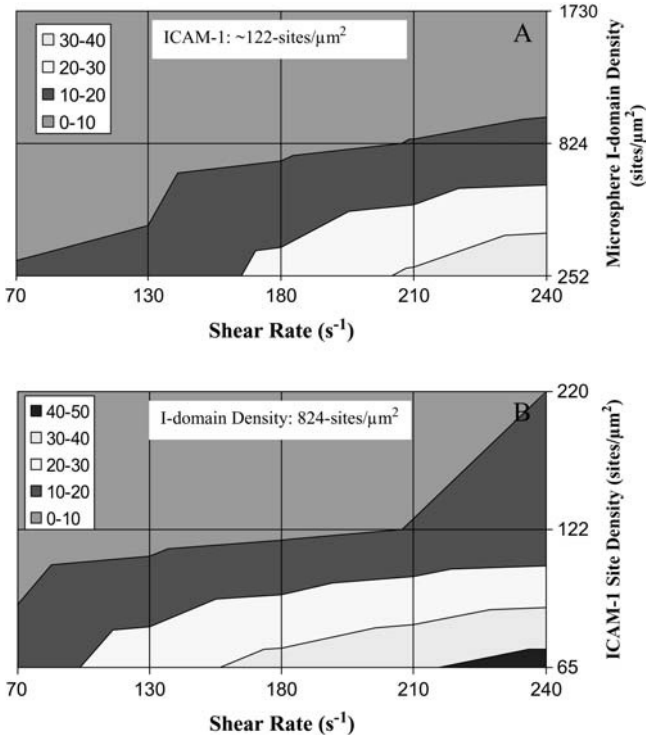

FIGURE 4 Contour plots showing the effect of (*A*) I-domain site density (at 1.25 μg/mL ICAM-1 coating) and (*B*) ICAM-1 substrate coating concentration (at 824 sites/μm^2 of I-domain) on microsphere rolling velocity sensitivity to wall shear stress in flow chamber. (*Legend*) Average microsphere rolling velocity range.

surfaces, respectively, but increased with a decrease in wall shear stress within the flow chamber. Similarly, the variation of rolling velocity with time decreases with decreasing wall shear stress and increasing I-domain and ICAM-1 densities. To quantify the fluctuations in rolling velocity, the root mean-squares (RMS) of the I-domain microsphere rolling velocity were calculated for the different molecular site densities and wall shear stresses studied. Fig. 6 shows plots of calculated average RMS rolling velocities for I-domain microspheres as a function of wall shear stress at different I-domain surface densities (*A*) and as a function of ICAM-1 substrate site density (*B*). As expected, average RMS rolling velocity significantly decreases with increase in microsphere I-domain site density at a single wall shear stress. Similarly, average RMS rolling velocity decreases with increasing ICAM-1 site density on the substrate surface. However, the effect of wall shear stress on the fluctuation in I-domain microsphere rolling velocity is not clear since there appears to be no clear trend seen with the calculated RMS velocity data at different shear stresses (Fig. 6 *A*). A plot of average RMS rolling velocity as a function of average microsphere rolling velocity for all conditions tested shows a linear relationship between RMS velocity and average rolling velocity (Fig. 6 *C*) similar to previously described (29).

AD simulations

By matching AD simulations to the comprehensive data set from these cell-free rolling experiments, we can estimate the Bell model parameters, k_r^0 and γ, of the wt I-domain-ICAM-1 bond. AD accounts for the experimental settings of flow shear rate, bead size, and adhesion molecule site densities of both flow chamber and beads. The intrinsic forward reaction rate, k_f^0, and the Bell model parameters remain as tunable inputs.

Initial simulations employed Bell model parameters for the resting LFA-1-ICAM-1 bond measured using atomic force microscopy, $k_r^0 = 4.0\,s^{-1}$ and $\gamma = 1.5$ Å (36); however, simulations using these values could not approximate the experimental data, despite manipulation of k_f^0. Noting that $k_r^0 = 4.0\,s^{-1}$ is of the same order of magnitude as BIAcore measurements of the reverse reaction rate for wt I-domain-ICAM-1 interactions ($5.55 \pm 0.65\ s^{-1}$) (18), we chose to hold k_r^0 fixed at this value. By allowing the reactive compliance as well as the forward rate to vary, we found a best fit to the experimental data using $k_f^0 = 0.1\,\mu m^2/s$, $k_r^0 = 4.0\,s^{-1}$, and $\gamma = 0.1$ Å (Fig. 7). These parameters are not strictly unique; rather, they are the best global fit to the experimental data. Values of k_f^0 between 0.2 and 0.4 μm^2/s, with γ held at 0.1 Å, provide fits of lesser quality. Values of k_f^0 beyond these bounds do not fit the data at all. With k_f^0 held at 0.3 μm^2/s, lesser quality fits result from values of γ ranging between 0.15 and 0.09 Å. Values of γ beyond these bounds do not fit the data.

Consistent with experiment, simulations did not demonstrate rolling within the experimental range of shear rates for beads coated with 94 I-domain sites/μm^2 (lowest bead site density) over a surface with 67 ICAM-1 sites/μm^2 (1.25 μg/mL ICAM-1-coated surface)(data not shown). Simulations of 94 sites/μm^2 I-domain beads flowing over surfaces of either 122 or 210 sites/μm^2 ICAM-1 (Fig. 7, *A* and *B*) demonstrated transient bead-surface interaction at 220 s^{-1} shear rate unlike experimental data (Fig. 3, *A* and *B*); however, the simulated bead rolling velocity was so high that corresponding experimental measurements would not have observed this behavior as rolling (data not shown).

Also in line with experimental measurements, the examination of instantaneous velocity of simulated beads shows that pause time decreases with increasing wall shear stress. A cell is considered to be paused when its velocity is $<1\%$ of the hydrodynamic velocity. Fig. 8 shows instantaneous rolling velocity traces of simulated microspheres rolling on 122 sites/μm^2 ICAM-1 surfaces as a function of shear rate and I-domain microsphere site density. Similar to experimental data shown in Fig. 5, *A* and *B*, the frequency of microsphere pauses decreases to zero as the shear rate increases from 70 s^{-1} (Fig. 8 *A*) to 180 s^{-1} (Fig. 8 *B*) for particles with 252 sites/μm^2 I-domain interacting with surfaces coated with 2.5 μg/ml. Also, average time paused by simulated microspheres increases with increase in I-domain and ICAM-1 site

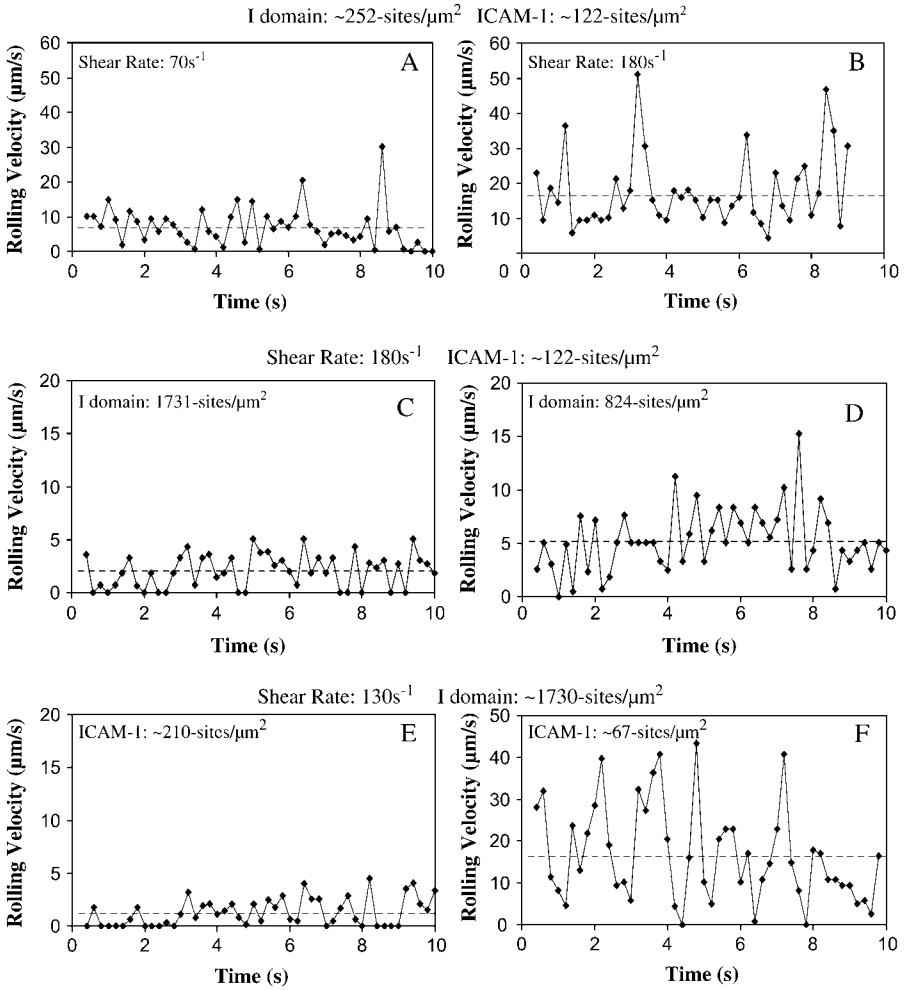

FIGURE 5 Comparison of instantaneous velocity traces of I-domain-coated SuperAvidin microspheres. Top panel compares traces for microspheres coated with 100% I-domain interacting with ICAM-1 surfaces (2.5 μg/mL coating) at shear rates of (*A*) 70 s^{-1} and (*B*) 210 s^{-1}. Middle panel compares traces of microspheres coated with (*C*) 100% and (*D*) 70% I-domain interacting with ICAM-1 surfaces (2.5 μg/mL coating) at a shear rate of 180 s^{-1}. Bottom panel compares traces of microspheres coated with 100% I-domain interacting on surfaces coated with (*E*) 5 μg/ml and (*F*) 1.25 μg/ml ICAM-1 at 130 s^{-1}.

densities on microspheres and substrate surfaces (data not shown), respectively. As an example, at 70 s^{-1} shear rate and 122 sites/μm^2 ICAM-1 site density, an increase in I-domain site density from 94 to 252 sites/μm^2 increases the percentage of time paused from 75% to 83%. Holding I-domain site density constant at 252 sites/μm^2, an increase in ICAM-1 site density from 122 to 210 further increases pause time to 95% (data not shown).

DISCUSSION

LFA-1 is the major adhesive molecule expressed on leukocytes involved in the firm adhesion of these cells to inflamed endothelium in vivo. This β_2-integrin binds to ICAMs on endothelial cells, after a switch to an active conformation mediated by signals from within transiently adhered cells. Recent work has focused on understanding the basis of LFA-1 affinity regulation and its effect on leukocyte adhesion. Particularly, researchers have focused on the I-domain of LFA-1 as the major domain involved in LFA-1 ligand binding, and these efforts have led to solving the crystal structure of LFA-1 I-domain (17,41). Molecular biology allows for the possibility of isolated expression of these molecules on cell surface to study their biophysical contribution(s) to leukocyte adhesion in inflammation. To this end, Springer and co-workers recently showed that the wt I-domain of LFA-1 and one locked in an open, high affinity conformation can, respectively, support rolling and firm adhesion of cells on ICAM-1 substrates in shear flow when expressed in $\alpha_L\beta_2$ heterodimers or as isolated domains on cell surfaces (10). However, this work and others (19) did not fully explore the ability of these molecules, particularly the wt I-domain, to mediate the capture of cells from free stream similar to selectin-mediated capture and rolling on leukocytes both in vitro and in vivo. Furthermore, to our knowledge, no work exists exploring the dynamics of rolling mediated by wt I-domain.

In this work, we present results from cell-free adhesion assays done to explore the potential ability of wt I-domain in mediating the capture and rolling of particles in flow at a range of shear stresses. This type of cell-free adhesion assay can allow for elucidating biophysical characteristics of I-domain-ICAM-1 interactions that are important in leukocyte adhesion, particularly through the control of I-domain

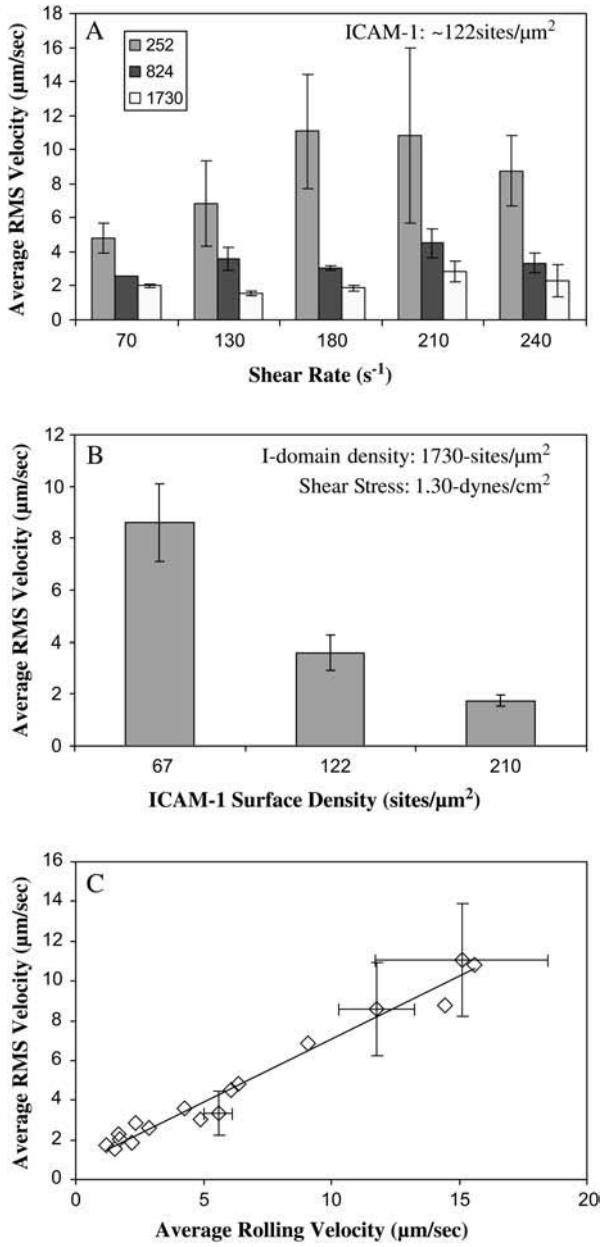

FIGURE 6 Average RMS velocities of microspheres ($n = 3$) (*A*) as a function of shear rate for particles with different I-domain site density interacting with surfaces coated with 2.5 μg/mL ICAM-1, (*B*) as a function of ICAM-1 substrate coating concentration for 100% I-domain particles (~1730 sites/μm) at 130 s^{-1}, and (*C*) as a function of average particle rolling velocity for all sites of I-domain and ICAM-1 densities tested at different wall shear stress. Error bar represents standard error calculations.

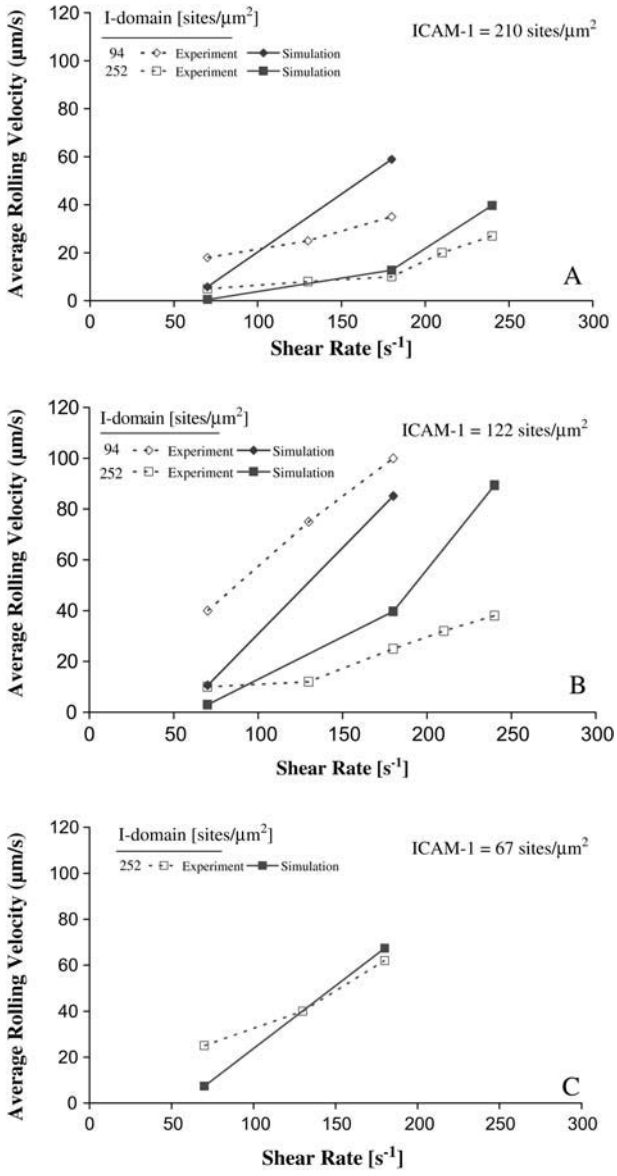

FIGURE 7 Simulated and experimental rolling velocity data for I-domain microspheres on (*A*) 210, (*B*) 122, and (*C*) 67 sites/μm^2 ICAM-1 surfaces. $\gamma = 0.1$ Å; $k_r^0 = 4\,s^{-1}$; and $k_f^0 = 0.3\,\mu m^2/s$. Error = standard deviation ($n \geq 7$).

surface density on the microspheres. Specifically, ~10 μm-sized polystyrene particles whose surfaces have been modified with wt I-domain were perfused over ICAM-1-coated surfaces in a parallel plate flow chamber. We show that, at all shear rates studied, wt I-domain can independently mediate the capture of polystyrene particles from flow when interacting with ICAM-1 surfaces, similar to selectin-ligand interaction and support-sustained rolling of microspheres on ICAM-1 surfaces. Contrary to previous work with wt I-domain expressed on cells by Springer and co-workers (10), I-domain microspheres did not firmly adhere to ICAM-1 substrate in all conditions tested. This could be due to differences in microspheres and cells' surface morphology and is not likely due to the differences in I-domain and LFA-1 since Salas et al. showed higher levels of firm adhesion for I-domain-expressing cells over those expressing an $\alpha_L\beta_2$ heterodimer in the presences of Ca^{2+} and Mg^{2+} (Fig. 3 in Salas et al. (10)). Furthermore, the presence of EDTA, a divalent ion chelator, in the perfusion buffer completely eliminated tethering and rolling of I-domain microspheres on ICAM-1 (Fig. 2), suggesting the presence

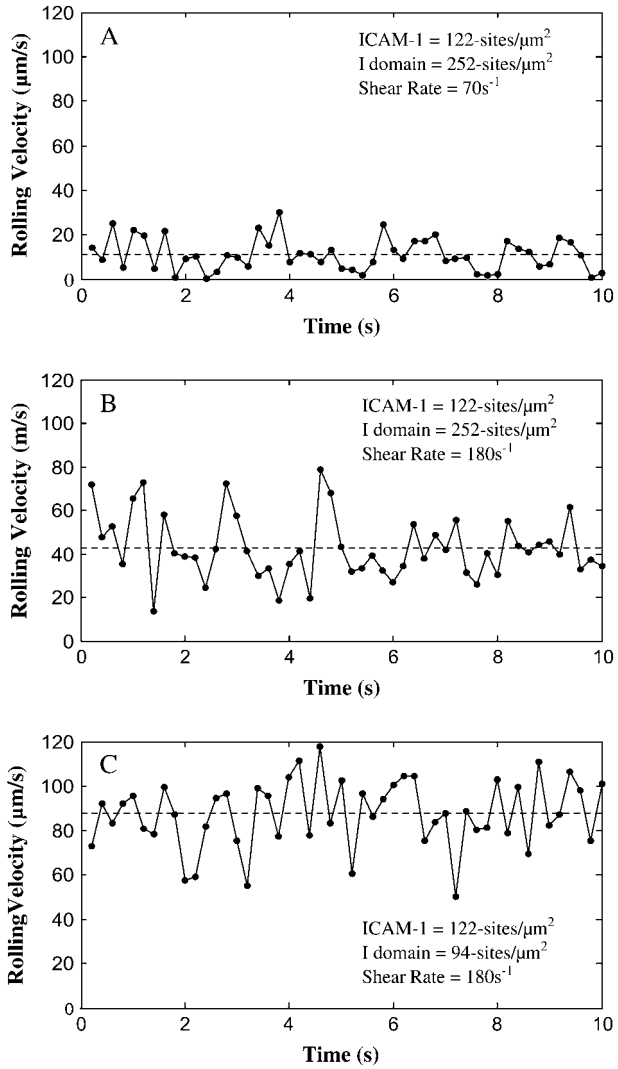

FIGURE 8 Effect of I-domain site density and shear stress on simulated bead instantaneous velocity distribution. Instantaneous velocity traces of simulated microspheres rolling on 122 sites/μm^2 ICAM-1 surfaces. Simulated microspheres with 252 sites/μm^2 I-domain interacting ICAM-1 at a shear rate of (*A*) 70 s^{-1} and (*B*) 180 s^{-1}. Panel *C* depicts a simulated trace for microspheres with 94 sites/μm^2 I-domain at 180 s^{-1} shear rate. $\gamma =$ 0.1 Å; $k_r^0 = 4\,s^{-1}$; $k_f^0 = 0.3\,\mu m^2/s$.

of divalent cations is necessary for I-domain-microsphere interactions, in agreement with previous publications (18,42). Experiments conducted with microspheres preincubated with the function-blocking antibody, TS2/6, at ~20 μg/mL show ~60% reduction in flux of rolling for microspheres coated with 1730 sites/μm^2 of I-domain (Fig. 2), and the particles that were rolling, in this case, did so with an average velocity that was 20 times faster (from 2.4 to 48 μm/s) than particles rolling in the absences of TS2/6. The lack of complete (100% reduction in flux) blocking of tethering by TS2/6 at ~20 μg/mL for beads with 1730 sites/μm^2 I-domain as reported in previous publications (10) suggests the use of a nonsaturating concentration of antibody. Limited supply of antibody prevented the use of higher concentrations for blocking experiments. However, we were able to show complete blocking of rolling interaction (~98% reduction in flux from a baseline of 264 bead/mm$^2\times$min) with the same concentration of TS2/6 when the amount of I-domain on microspheres was reduced by ~½ (824 sites/μm^2) (Fig. 2). Overall, the magnitude of rolling velocities obtained with I-domain microspheres in this work were in the range (0–60 μm/s), similar to previously obtained for wt I-domain expressed on K562 cells (10).

Previous work with cell-expressed wt I-domain interacting with ICAM-1 substrate from flow show that rolling velocity of these cell increases with increasing wall shear stress; however, these authors did not explore the effect of I-domain density (or ICAM-1 density) on rolling (10,19). As previously shown with selectin-mediated rolling, I-domain microspheres' rolling interactions depend on wall shear stress within the flow chamber, as well as receptor (I-domain) and ligand (ICAM-1) density on microsphere and substrate surfaces, respectively (21,29). The effect of wall shear on rolling velocity appears to be coupled to the molecule site density. In Fig. 4, we show that at the highest density of I-domain (~1700 sites/μm^2) on microsphere surfaces and ICAM-1 density on substrate surfaces (~210 sites/μm^2), microsphere rolling velocity appears to be insensitive to wall shear stress (Fig. 4 *A*). However, at low I-domain or ICAM-1 densities or a combination of both (Fig. 4 *C*), microsphere rolling velocities show more sensitivity to shear stress, where velocity increased linearly with an increase in wall shear stress over the range of shear stresses studied. At intermediate level of I-domain and ICAM-1 densities, there exist two regimes where the sensitivity of rolling velocity to wall shear stress is different—one of low sensitivity to an increase in shear stress occurring at low wall shear stress and the other of high sensitivity to increase in shear stress occurring at higher wall shear stresses within the flow chamber (see *squares* in Fig. 4). This observation is also consistent with the rolling interaction seen with cell-expressed I-domain or $\alpha_L\beta_2$, where multiple slopes exist in the plot of rolling velocities as a function of shear stress (10). Overall, the data present in Fig. 4 suggest that at the highest I-domain and ICAM-1 densities, there exists an excess of I-domain-ICAM-1 bonds in the contact region to withstand the counteracting force from flow over the range of shear stresses studied.

Instantaneous rolling provides another way of characterizing the rolling dynamics of wt I-domain-coated microspheres on ICAM-1 substrates. Results presented in Fig. 6 show that microspheres displayed pause interactions when interacting with ICAM-1 substrates in flow, similar to what has been previously described for selectin-mediated rolling of neutrophils in flow (21). We also show that the potential for pause interaction seen with I-domain microspheres is a function of molecular density and wall shear stress, suggesting that these pauses are due to receptor-ligand interaction, rather than nonspecific interaction between polystyrene

microspheres and substrate surfaces. Similarly, analysis of the RMS rolling velocity data, as described in a previous publication (29), shows I-domain microspheres rolling with varying velocity on ICAM-1-coated surfaces. Furthermore, fluctuation in rolling velocity with time increases with a decrease in microsphere and substrate I-domain and ICAM-1 density, respectively (Fig. 7), similar to fluctuations seen in selectin-mediated rolling of particles in flow (21,29). Once again, this observation suggests that fluctuation in rolling velocity with time is a result of fluctuation in I-domain-ICAM-1 binding, in agreement with previous predictions by Hammer and Apte using dynamics simulation (30). A plot of RMS rolling velocities as a function of average particle rolling velocity for all conditions tested shows a linear relationship between these two parameters, suggesting that rolling velocity sets fluctuations in rolling, i.e., measurement of the rolling velocity of a particle can predict the magnitude of fluctuation in rolling velocity for that particle (Fig. 6 *C*).

Results from AD simulation of I-domain-ICAM-1 rolling interactions show a good correlation with experimental data and suggest an off rate and reactive compliance for I-domain-ICAM-1 interactions of 4 s^{-1} and 0.1 Å, respectively. These values are within the same magnitude of values determined for selectin-carbohydrate interaction, suggesting a rolling behavior of I-domain particles on ICAM-1 substrates as seen with experiments (22). As with experiments, AD shows fluctuation in rolling velocity and the amount of time paused that increases with wall shear stress and I-domain and ICAM-1 microspheres and substrate density, respectively (Fig. 8).

The important role of molecular densities in prescribing rolling dynamics of I-domain-coated microspheres further highlights the importance of I-domain (LFA-1) expression level in the ability of this molecule to support rolling adhesion in vivo. Work by Alon and co-workers shows that LFA-1-mediated rolling is independent of ligand affinity to LFA-1 but rather dependent on an affinity-independent mechanism of integrin clustering (20). In this work, we show an absence of tethering or rolling of microspheres at a combination of very low I-domain (94 sites/μm^2) and ICAM-1 ($\sim$67 sites/μm^2) densities, supporting the idea that low avidity of LFA-1 rather than affinity to ICAM-1 might prevent the ability of this integrin to mediate in vivo tethering of leukocytes in the absence of selectin-carbohydrate interaction.

Finally, work exists in the literature that suggests the contribution of β_2-integrin to selectin-mediated rolling—where leukocytes are observed to display faster rolling in the absence of β_2-integrin interactions (13,19). The observed similarity in the dynamics of cell-free I-domain rolling adhesion on ICAM-1 described here to that of previously published selectin-mediated rolling further highlight the possibility that the I-domain of LFA-1 in its inactive state contributes to the capture and rolling of neutrophils in vivo. Furthermore, evidence in the literature suggests that LFA-1 is the important β_2-integrin involved in the in vivo transition of leukocytes from rolling to firm adhesion (14,43). Also, previous work in our laboratory showed that the transition from selectin-mediated rolling to β_2-integrin-mediated firm binding occurs in a gradual process when particles co-functionalized with the rolling ligand, sLe^X, and an antibody to ICAM-1 with similar binding kinetics to active LFA-1 were allowed to interact with surfaces coated with both selectin and ICAM-1 in flow (27). In this previously described cell-free work, we showed that ICAM-1-antibody interactions also slow rolling similar to ICAM-1-β_2-integrin interaction in vivo and that selectin-carbohydrate interaction was necessary for optimum firm binding mediated by the antibody-ICAM-1 interactions. It is possible that this type of interplay between leukocyte rolling and firm adhesion in itself could serve as a dynamic regulation for the system of adhesion seen with leukocytes, and work by Simon and co-workers, where rolling neutrophils on E-selectin transition to firmly adherent cells in the absence of chemotactic stimulation, allude to this fact (44). Moreover, Springer and co-workers (22) previously suggested that force (from tethering) alone is sufficient to shift the conformation of wt I-domain toward the open, high affinity conformation, thereby increasing its affinity to ICAM-1 (10). Furthermore, they recently showed that the extension of $\alpha_L\beta_2$ is critical for the rolling and firm binding supported by this molecule (45). All together, this suggests that selectin-mediated rolling supported by LFA-1 (β_2-integin) transient interactions can allow for enough force from flow that results in the transition of LFA-1 to its active state to support the firm arrest of these cells to the endothelium. Work is underway to characterize the adhesion of particles functionalized with the I-domain of LFA-1 locked in the open position that mimics the active state of the molecule in vivo and to understand how selectins and I-domain might act in synergy to support rolling and firm adhesion. Overall, we believe the cell-free adhesion system presented in this work can be adapted to fit cell systems to further elucidate the role of LFA-1 and its adhesion domains in leukocyte interaction with endothelial cells during inflammation response.

Special thanks to Ms. Natalie Aaronson for her technical assistance.

We acknowledge funding from NIH-EB-00256 and HL-18208, NASA Graduate Student Researcher Program (A.O.E.), and Medical Student Training Program from the University of Pennsylvania (E.F.K.).

REFERENCES

1. Springer, T. A. 1994. Traffic signals for lymphocyte recirculation and leukocyte emigration: the multistep paradigm. *Cell.* 76:301–314.
2. Lawrence, M. B., and T. A. Springer. 1991. Leukocytes roll on a selectin at physiologic flow rates: distinction from and prerequisite for adhesion through integrins. *Cell.* 65:859–873.
3. Tonnesen, M. G. 1989. Neutrophil-endothelial cell interactions: mechanisms of neutrophil adherence to vascular endothelium. *J. Invest. Dermatol.* 93:53S–58S.
4. Gopalan, P. K., C. W. Smith, H. Lu, E. L. Berg, L. V. McIntire, and S. I. Simon. 1997. Neutrophil CD18-dependent arrest on intercellular

adhesion molecule 1 (ICAM-1) in shear flow can be activated through L-selectin. *J. Immunol.* 158:367–375.

5. Stewart, M. P., C. Cabanas, and N. Hogg. 1996. T cell adhesion to intercellular adhesion molecule-1 (ICAM-1) is controlled by cell spreading and the activation of integrin LFA-1. *J. Immunol.* 156:1810–1817.
6. Doerschuk, C. M., S. Tasaka, and Q. Wang. 2000. CD11/CD18-dependent and -independent neutrophil emigration in the lungs: how do neutrophils know which route to take? *Am. J. Respir. Cell Mol. Biol.* 23:133–136.
7. O'Brien, C. D., P. Lim, J. Sun, and S. M. Albelda. 2003. PECAM-1-dependent neutrophil transmigration is independent of monolayer PECAM-1 signaling or localization. *Blood.* 101:2816–2825.
8. Riaz, A. A., M. X. Wan, T. Schaefer, R. Schramm, H. Ekberg, M. D. Menger, B. Jeppsson, and H. Thorlacius. 2002. Fundamental and distinct roles of P-selectin and LFA-1 in ischemia/reperfusion-induced leukocyte-endothelium interactions in the mouse colon. *Ann. Surg.* 236:777–784 (discussion 784).
9. Butcher, E. C., and L. J. Picker. 1996. Lymphocyte homing and homeostasis. *Science.* 272:60–66.
10. Salas, A., M. Shimaoka, S. Chen, C. V. Carman, and T. A. Springer. 2002. Transition from rolling to firm adhesion is regulated by the conformation of the I domain of the integrin LFA-1. *J. Biol. Chem.* 277: 50255–50262.
11. Jung, U., K. E. Norman, K. Scharffetter-Kochanek, A. L. Beaudet, and K. Ley. 1998. Transit time of leukocytes rolling through venules controls cytokine-induced inflammatory cell recruitment in vivo. *J. Clin. Invest.* 102:1526–1533.
12. Kunkel, E. J., U. Jung, D. C. Bullard, K. E. Norman, B. A. Wolitzky, D. Vestweber, A. L. Beaudet, and K. Ley. 1996. Absence of trauma-induced leukocyte rolling in mice deficient in both P-selectin and intercellular adhesion molecule 1. *J. Exp. Med.* 183:57–65.
13. Steeber, D. A., M. A. Campbell, A. Basit, K. Ley, and T. F. Tedder. 1998. Optimal selectin-mediated rolling of leukocytes during inflammation in vivo requires intercellular adhesion molecule-1 expression. *Proc. Natl. Acad. Sci. USA.* 95:7562–7567.
14. Dunne, J. L., C. M. Ballantyne, A. L. Beaudet, and K. Ley. 2002. Control of leukocyte rolling velocity in TNF-alpha-induced inflammation by LFA-1 and Mac-1. *Blood.* 99:336–341.
15. Henderson, R. B., L. H. Lim, P. A. Tessier, F. N. Gavins, M. Mathies, M. Perretti, and N. Hogg. 2001. The use of lymphocyte function-associated antigen (LFA)-1-deficient mice to determine the role of LFA-1, Mac-1, and alpha4 integrin in the inflammatory response of neutrophils. *J. Exp. Med.* 194:219–226.
16. Humphries, M. J. 2000. Integrin structure. *Biochem. Soc. Trans.* 28: 311–339.
17. Qu, A., and D. J. Leahy. 1995. Crystal structure of the I-domain from the CD11a/CD18 (LFA-1, alpha L beta 2) integrin. *Proc. Natl. Acad. Sci. USA.* 92:10277–10281.
18. Shimaoka, M., C. Lu, R. T. Palframan, U. H. von Andrian, A. McCormack, J. Takagi, and T. A. Springer. 2001. Reversibly locking a protein fold in an active conformation with a disulfide bond: integrin alphaL I domains with high affinity and antagonist activity in vivo. *Proc. Natl. Acad. Sci. USA.* 98:6009–6014.
19. Knorr, R., and M. L. Dustin. 1997. The lymphocyte function-associated antigen 1 I domain is a transient binding module for intercellular adhesion molecule (ICAM)-1 and ICAM-3 in hydrodynamic flow. *J. Exp. Med.* 186:719–730.
20. Sigal, A., D. A. Bleijs, V. Grabovsky, S. J. Van Vliet, O. Dwir, C. G. Figdor, Y. van Kooyk, and R. Alon. 2000. The LFA-1 integrin supports rolling adhesions on ICAM-1 under physiological shear flow in a permissive cellular environment. *J. Immunol.* 165:442–452.
21. Rodgers, S. D., R. T. Camphausen, and D. A. Hammer. 2000. Sialyl Lewis(x)-mediated, PSGL-1-independent rolling adhesion on P-selectin. *Biophys. J.* 79:694–706.
22. Chang, K. C., D. F. Tees, and D. A. Hammer. 2000. The state diagram for cell adhesion under flow: leukocyte rolling and firm adhesion. *Proc. Natl. Acad. Sci. USA.* 97:11262–11267.
23. Springer, T. A., D. Davignon, M. K. Ho, K. Kurzinger, E. Martz, and F. Sanchez-Madrid. 1982. LFA-1 and Lyt-2,3, molecules associated with T lymphocyte-mediated killing; and Mac-1, an LFA-1 homologue associated with complement receptor function. *Immunol. Rev.* 68: 171–195.
24. Sanchez-Madrid, F., A. M. Krensky, C. F. Ware, E. Robbins, J. L. Strominger, S. J. Burakoff, and T. A. Springer. 1982. Three distinct antigens associated with human T-lymphocyte-mediated cytolysis: LFA-1, LFA-2, and LFA-3. *Proc. Natl. Acad. Sci. USA.* 79: 7489–7493.
25. Altman, J. D., P. A. Moss, P. J. Goulder, D. H. Barouch, M. G. McHeyzer-Williams, J. I. Bell, A. J. McMichael, and M. M. Davis. 1996. Phenotypic analysis of antigen-specific T lymphocytes. *Science.* 274:94–96.
26. Schatz, P. J. 1993. Use of peptide libraries to map the substrate specificity of a peptide-modifying enzyme: a 13 residue consensus peptide specifies biotinylation in Escherichia coli. *Biotechnology (N. Y.).* 11:1138–1143.
27. Crawford, F., H. Kozono, J. White, P. Marrack, and J. Kappler. 1998. Detection of antigen-specific T cells with multivalent soluble class II MHC covalent peptide complexes. *Immunity.* 8:675–682.
28. Eniola, A. O., P. J. Willcox, and D. A. Hammer. 2003. Interplay between rolling and firm adhesion elucidated with a cell-free system engineered with two distinct receptor-ligand pairs. *Biophys. J.* 85: 2720–2731.
29. Eniola, A. O., S. D. Rodgers, and D. A. Hammer. 2002. Characterization of biodegradable drug delivery vehicles with the adhesive properties of leukocytes. *Biomaterials.* 23:2167–2177.
30. Brunk, D. K., and D. A. Hammer. 1997. Quantifying rolling adhesion with a cell-free assay: E-selectin and its carbohydrate ligands. *Biophys. J.* 72:2820–2833.
31. Hammer, D. A., and S. M. Apte. 1992. Simulation of cell rolling and adhesion on surfaces in shear flow: general results and analysis of selectin-mediated neutrophil adhesion. *Biophys. J.* 63:35–57.
32. King, M. R., and D. A. Hammer. 2001. Multiparticle adhesive dynamics: hydrodynamic recruitment of rolling leukocytes. *Proc. Natl. Acad. Sci. USA.* 98:14919–14924.
33. Goldman, A. J., R. G. Cox, and H. Brenner. 1967. Slow viscous motion of a sphere parallel to a plane wall. I. Motion through a quiescent fluid. *Chem. Eng. Sci.* 22:637–652.
34. Goldman, A. J., R. G. Cox, and H. Brenner. 1967. Slow viscous motion of a sphere parallel to a plane wall. II. Couette flow. *Chem. Eng. Sci.* 22:653–659.
35. Bell, G. I. 1978. Models for specific adhesion of cells to cells. *Science.* 200:618–627.
36. Zhang, X. H., E. Wojcikiewicz, and V. T. Moy. 2002. Force spectroscopy of the leukocyte function-associated antigen-1/intercellular adhesion molecule-1 interaction. *Biophys. J.* 83:2270–2279.
37. Bell, G. I., M. Dembo, and P. Bongrand. 1984. Cell adhesion. Competition between nonspecific repulsion and specific bonding. *Biophys. J.* 45:1051–1064.
38. Chang, K. C., and D. A. Hammer. 1999. The forward rate of binding of surface-tethered reactants: effect of relative motion between two surfaces. *Biophys. J.* 76:1280–1292.
39. Thiel, M., C. Zourelidis, J. D. Chambers, U. H. von Andrian, K. E. Arfors, K. Messmer, and K. Peter. 1997. Expression of beta 2-integrins and L-selectin on polymorphonuclear leukocytes in septic patients. *Eur. Surg. Res.* 29:160–175.
40. Edwards, B. S., M. S. Curry, H. Tsuji, D. Brown, R. S. Larson, and L. A. Sklar. 2000. Expression of P-selectin at low site density promotes selective attachment of eosinophils over neutrophils. *J. Immunol.* 165:404–410.
41. Legge, G. B., R. W. Kriwacki, J. Chung, U. Hommel, P. Ramage, D. A. Case, H. J. Dyson, and P. E. Wright. 2000. NMR solution structure of the inserted domain of human leukocyte function associated antigen-1. *J. Mol. Biol.* 295:1251–1264.

42. Lu, C., M. Shimaoka, M. Ferzly, C. Oxvig, J. Takagi, and T. A. Springer. 2001. An isolated, surface-expressed I domain of the integrin alphaLbeta2 is sufficient for strong adhesive function when locked in the open conformation with a disulfide bond. *Proc. Natl. Acad. Sci. USA*. 98:2387–2392.

43. Hentzen, E. R., S. Neelamegham, G. S. Kansas, J. A. Benanti, L. V. McIntire, C. W. Smith, and S. I. Simon. 2000. Sequential binding of CD11a/CD18 and CD11b/CD18 defines neutrophil capture and stable adhesion to intercellular adhesion molecule-1. *Blood*. 95:911–920.

44. Simon, S. I., Y. Hu, D. Vestweber, and C. W. Smith. 2000. Neutrophil tethering on E-selectin activates beta 2 integrin binding to ICAM-1 through a mitogen-activated protein kinase signal transduction pathway. *J. Immunol*. 164:4348–4358.

45. Salas, A., M. Shimaoka, A. N. Kogan, C. Harwood, U. H. von Andrian, and T. A. Springer. 2004. Rolling adhesion through an extended conformation of integrin alphaLbeta2 and relation to alpha I and beta I-like domain interaction. *Immunity*. 20:393–406.

46. Brunk, D. K., D. J. Goetz, and D. A. Hammer. 1996. Sialyl Lewis(x)/E-selectin-mediated rolling in a cell-free system. *Biophys. J*. 71:2902–2907.

47. Patel, K. D., M. U. Nollert, and R. P. McEver. 1995. P-selectin must extend a sufficient length from the plasma membrane to mediate rolling of neutrophils. *J. Cell. Biol*. 131:1893–1902.

48. Morozov, V. N., and T. Y. Morozova. 1990. What does a protein molecule look like? *Commun. Mol. Cell. Biophys*. 6:249–270.